PAPER

Check for updates

The toxicity, uptake, and impact on galectin-3 mediated apoptosis of lactose functionalized PAMAM dendrimers†

Mackenzie S. Fricke,‡[a] Magalee R. Frometa,‡[a] Yannic Kerkhoff,[bc] Samuel P. Bernhard,[a] Ramat S. Tahir,[a] Elisa Quaas,[b] William H. Totten,[a] Rainer Haag, [ID][b] Katharina Achazi [ID][b] and Mary J. Cloninger *[a]

Poly(amidoamine) (PAMAM) dendrimers functionalized with ligands that are designed to interact with biological receptors are important macromolecules for the elucidation and mediation of biological recognition processes. Specifically, carbohydrate functionalized dendrimers are useful synthetic multivalent systems for the study of multivalent protein–carbohydrate interactions. For example, lactose functionalized glycodendrimers can be used to discern the function of galectins, galactoside-binding proteins that are often over-expressed during cancer progression. In order to effectively interpret cancer cellular assays using glycodendrimers, however, their properties in the presence of cells must first be assessed. Macromolecules that are taken up by cells would be expected to have access to many different cell signaling pathways and modes of action that solely extracellular macromolecules cannot utilize. In addition, macromolecules that display cellular toxicity could not be used as drug delivery vehicles. Here, we report fundamental studies of cellular toxicity, viability, and uptake with four generations of lactose functionalized PAMAM dendrimers. In all cases, the dendrimers are readily taken up by the cells but do not display any significant cellular toxicity. The glycodendrimers also increase cellular apoptosis, suggesting that they may abrogate the antiapoptotic protections afforded by galectin-3 to cancer cells. The results reported here indicate that appropriately functionalized PAMAM dendrimers can be used as nontoxic tools for the study and mediation of both extra and intracellular cancer processes.

Introduction

Many biological processes are mediated by glycan–lectin interactions that induce signal transduction. One of the first such discoveries by Nowell showed that lectins from red kidney beans could induce mitosis in lymphocytes.[1,2] Since then, many studies have reported on the influence of cell-surface carbohydrates binding to their receptor lectins.[3–5] Although most of these carbohydrate–lectin interactions are relatively weak, protein–carbohydrate interactions heavily influence biological processes such as glycan mediated cell attachment and endocytosis of a virus.[6,7] To enhance the selectivity and specificity of

weak carbohydrate-mediated interactions, nature commonly invokes multivalency. In multivalent interactions, multiple ligands bind to multiple receptors, synergistically enhancing the overall binding avidity of the system.[8–11]

To investigate a multivalent system for the display of carbohydrates, we and others have utilized lactose functionalized dendrimers.[12–22] The poly(amidoamine) (PAMAM) dendrimers used herein are highly branched macromolecules with repeating amidoamine units emanating from a central core.[23–25] When the amino endgroups are functionalized with lactosides *via* a thiourea linkage, the dendrimers present a multivalent carbohydrate ligand display appropriate for the study of carbohydrate mediated multivalent interactions. The dendrimers used for this study are shown in Fig. 1, with characterization data provided in Table 1.[14]

Glycodendrimers are important macromolecules for the study and mediation of protein–carbohydrate interactions that, while known to be important, are often poorly understood.[20,26–33] Glycodendrimers are particularly attractive for the study of galectins, or beta-galactoside binding proteins, which play important

[a] Department of Chemistry and Biochemistry, Montana State University, Bozeman, MT, 59717, USA. E-mail: mcloninger@montana.edu

[b] Institut für Chemie und Biochemie, Freie Universität Berlin, Takustr. 3, 14195 Berlin, Germany

[c] IT and Data Services, Zuse Institute Berlin, Takustr. 7, 14195 Berlin, Germany

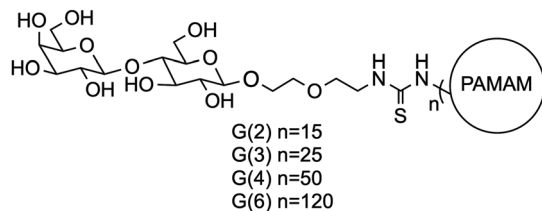† Electronic supplementary information (ESI) available. See DOI: https://doi.org/10.1039/d4ma00782d

‡ Shared first authorship.

Fig. 1 Schematic representation of the lactose functionalized PAMAM dendrimers used in this report.

G(2) n=15
G(3) n=25
G(4) n=50
G(6) n=120

Table 1 Characteristics of lactose functionalized PAMAM dendrimers

Glycoden. generation	$M_w{}^a$ (kDa)	Lactose endgroups	$R_h{}^b$ (nm)	Mobility^c (μm cm V^{-1} s^{-1})	Zeta potential^c (mV)
G(2)	10.3	15	1.8 ± 0.4	0.00 ± 0.01	0.1 ± 0.2
G(3)	18.7	25	2.5 ± 0.1	0.01 ± 0.01	0.2 ± 0.3
G(4)	37.8	50	2.9 ± 0.2	-0.01 ± 0.01	-0.1 ± 0.2
G(6)	114.6	120	5.1 ± 0.3	-0.01 ± 0.02	-0.1 ± 0.3
G(6)	58.0	0	4.4 ± 0.2	0.33 ± 0.03	6.9 ± 0.8

^{a} Weighted mass averages (M_w) were determined by MALDI-TOF. ^{b} Hydrodynamic radii (R_h) were determined by DLS in PBS. ^{c} Electrophoretic mobilities and zeta potentials were determined by PALS at 10 mM in Millipore water.

roles in many intercellular recognition processes including pathogen recognition and cancer progression.[5,34–37] Moreover, the burgeoning identification of the importance of intracellular galectins in processes including apoptosis also necessitates development of probes that can be taken up by cells.[37,38] Formation of lattices on the cell surface prolongs the residence time of galectins at the surface, while glycolipid–lectin, caveolae, clathrin, and lipid-raft mediated pathways facilitate endocytosis of galectins and glycopolymers.[39,40] Thus, in order to meaningfully interpret assay data for studies using glycodendrimers with galectins, information about properties such as cellular uptake and toxicity must be elucidated.

A variety of synthetic multivalent frameworks functionalized with ligands that bind to galectins have been reported to be taken up by cells. For example, glycocalix[4]arenes bearing 3′-O-coumarylmethyllactosides,[41] glycopolymers bearing 3′-O and 3-O aromatic thiodigalactosides,[42] beta-cyclodextrins with appended lactosides,[43] galactose functionalized polymer-containing nanoparticles,[44] and lactose functionalized PAMAM dendrimers bearing alpha-cyclodextrins[45] have all been shown to be taken up by mammalian cells. This is important because macromolecules capable of penetrating the cell could induce intracellular interactions with galectins *via* mechanisms unavailable to compounds that are solely extracellular. When using cell-based assays to study multivalent galectin–carbohydrate interactions, different interpretations of assay results must be considered depending on whether the glycodendrimers remain in the extracellular space or are endocytosed. Here, we report that all four generations of lactose functionalized PAMAM dendrimers shown in Fig. 1 are nontoxic and are taken up by cancer cells, indicating that both intracellular and extracellular

galectin-mediated processes can be targeted using even relatively large glycodendrimers.

Because galectin-3 has been reported to play a very important role in protecting cancer cells from apoptosis pathways, but the mechanisms of action are not well understood, use of intracellular glycodendrimers to study galectin-3 mediated apoptosis is highly desirable.[46,47] Apoptosis is highly regulated and is a mediator of anti-inflammatory processes; activating apoptosis in cancer cells is a difficult task since many cancers have deleted or altered expression of apoptosis regulating proteins. Galectin-3 has been proposed to bind to Bax (Bcl-2 associated $\times$ protein) to regulate intrinsic apoptosis, and multivalent binding of a very large modified citrus pectin glycopolymer called GCS-100 (molecular weight up to 250 kDa) was proposed as a method to disrupt this interaction.[48,49] Unlike the other galectins, galectin-3 possesses a non-carbohydrate-binding N-terminal domain that allows galectin-3 to oligomerize, causing the receptor function to be multivalent.[50–53] When galectin-3 and lactose functionalized dendrimers associate, a host of multivalent cross-linking interactions and consequences are enabled.[54–57] Here, we demonstrate that the lactose functionalized glycodendrimers can induce a small amount of cancer cellular apoptosis. Moreover, addition of galectin-3 with the glycodendrimers abrogates the observed effect of the glycodendrimers on apoptosis. This suggests that nontoxic glycodendrimers can bind galectin-3 and reduce the antiapoptotic effect of galectin-3.

In addition to apoptosis, galectin-3 (like many of the galectins) is also involved in many other cancer processes including angiogenesis, tumour formation, and cancer cellular migration and metathesis.[46,58–60] The lactose functionalized PAMAM dendrimers tested here are highly desirable tools for the study of both intracellular and extracellular galectin mediated processes involved in cancer progression. The toxicity, uptake, and apoptosis studies reported here afford a greater understanding of the properties of glycodendrimers. Specifically, lactose functionalized PAMAM dendrimers are nontoxic, are readily taken up by cancer cells, and the results reported here are broadly important for the design of new materials, including dendrimers, to study galectin mediated cellular processes.

Experimental section

Materials

General reagents were purchased from Millipore Sigma and Thermo Scientific Chemical Companies. PAMAM dendrimers were purchased from Dendritech. Alexafluor 647 hydrazide and cell staining reagents were obtained from Thermo Fisher Scientific. Zeba spin desalting columns (5 mL, 40 kDa and 7 kDa MWCO) and Sartorius Vivaspin Turbo PES centrifugal filters with 3000 and 10 000 MWCOs were purchased from Avantor/VWR. The Apotox-Glo Triplex Assay was purchased from Promega. Lactose functionalized PAMAM dendrimers were synthesized according to published procedures.[14] Phosphate buffered saline (PBS) is 1$\times$ diluted from the Cold Spring Harbor 10$\times$ PBS protocol.

Cell culture

DU-145 (ATCC: HTB-81) prostate carcinomas were cultured in media consisting of Dulbecco's Modified Eagle's Medium (DMEM: Gibco, 61100) with 1.8 g L^{-1} NaHCO$_3$ and supplemented with MEM vitamin (Gibco, 11126), Penn/strep (Gibco, 15140), NEAA (Gibco, 11140), EAA (Gibco, 11130), and 10% v/v fetal bovine serum (FBS). A549 (ATCC: CCL-185) lung carcinomas were cultured in F-12K Medium (Kaighn's Modification of Ham's F-12 Medium, ATCC: 30-2004) supplemented with Penn/strep (Gibco, 15140) and 10% v/v fetal bovine serum (FBS). For flow cytometry and confocal microscopy, A549 cells were cultured in DMEM supplemented with 2% glutamine, 100 U mL^{-1} penicillin, 100 µg mL^{-1} streptomycin (all from Gibco BRL), and 10% fetal calf serum (Thermo Fisher) at 37 °C and 5% CO$_2$. HT-1080 (ATCC: CCL-121) fibrosarcomas were cultured in media consisting of Dulbecco's Modified Eagle's Medium (DMEM: Gibco, 61 100) with 1.8 g L^{-1} NaHCO$_3$ and supplemented with MEM vitamin (Gibco, 11126), Penn/strep (Gibco, 15140), NEAA (Gibco, 11140), EAA (Gibco, 11130) and 5% v/v fetal bovine serum (FBS). Cells were cultured in a humidified incubator with 5% CO$_2$ and 37 °C. Before confluency, cells were subcultured using 0.25% (w/v) trypsin–0.53 mM EDTA.

Toxicity assay

Whole media was poured off cells, which were then covered in 0.25% trypsin and 0.02% EDTA solution and incubated for 4 min. Cells were gently aspirated using a disposable pipette, collected in a 15 mL falcon tube and centrifuged for 5 min at 2000 rpm. Trypsin/EDTA solution was poured off and the cell pellet was resuspended in 1 mL whole media. 10 µL cell solution was transferred to a sterile tube and diluted with 90 µL media and mixed. 10 µL of this solution was transferred to another sterile tube and combined with 10 µL Trypan Blue. 10 µL of this cell/dye solution was placed on a hemocytometer, and cells were counted to determine total cell count. From this count, the cells were diluted to a 200 000 cells per mL solution with whole media. Two solutions of controls were made from this cell solution: toxic control and viable control. The viable control contained cell solution with Celltox dye at a ratio of 1 : 500 in whole media. Toxic control contained cell solution, Celltox lysis solution in 1 : 25, and Celltox dye at 1 : 500. A media control was made with whole media and Celltox dye at 1 : 1000. Dendrimer solutions were concentrated to 8 mg mL^{-1} in whole media. In 96 well plates, the solutions were aliquoted with six replicates. Total volume in each well was 100 µL. For each of the dendrimer wells, 50 µL of dendrimer solution was combined with 50 µL of viable cells; final concentrations of glycodendrimers per well were as follows. G(2): 390 µM, G(3): 190 µM; G(4): 90 µM, G(6): 35 µM. For the toxic control wells: 50 µL toxic control solution was combined with 50 µL of whole media. The viable control wells: 50 µL viable cell solution (1 : 500 celltox dye with 200 000 cells per mL) and 50 µL of whole media. Media control wells: 100 µL media control solution. Plate was covered with foil to protect dye from light and placed in an incubator at 37 °C, 5% CO$_2$. At 2 and 24 h, the plate was removed from the

incubator, and fluorescence was recorded using a Biotek hybrid 1 plate reader at $485_{Ex}/520_{Em}$ nm. Six replicates were performed.

Synthesis of Alexafluor 647 functionalized glycodendrimers

Glycodendrimers were weighed (4 mg for G(2), 4.2 mg for G(3), 3.6 mg for G(4), and 3.3 mg for G(6)) and each dissolved with DI water for a final concentration of 2 mg mL^{-1}. An aqueous stock solution of 2 mg mL^{-1} NaIO$_4$ was prepared, and 2 equiv./dendrimer was added to each dendrimer solution and allowed to stir for 2 h in the dark. Reaction concentrations of NaIO$_4$ were as follows: 83 µL for G(2), 64 µL for G(3), 21 µL for G(4), and 4 µL for G6. NaIO$_4$ was then removed from the dendrimer solution using a centrifugal concentrator (MWCO of 3 kDa for G(2) and G(3) and 10 kDa for G(4) and G(6)). The NaIO$_4$ solution was displaced by adding 2 mL of a sodium acetate buffer (pH 5.5). G(2) and G(3) were centrifuged 4 times at 4000 × g for 60 min per spin. G(4) and G(6) were centrifuged 4 times at 2000 × g for 60 min per spin. Once the aldehyde intermediates were in sodium acetate buffer, Alexafluor 647 dye (1 mg, hydrazide) was dissolved in 500 µL of the sodium acetate buffer and was added to each reaction vial (1 equiv./dendrimer; 197 µL for G(2), 154 µL for G(3), 50 µL for G(4), and 15 µL for G(6)). The vials were incubated in the dark for 24 h at 4 °C, purified *via* SEC spin column (G(2) and G(3) used a spin column with a MWCO of 7 kDa, and G(4) and G(6) used a MWCO of 40 kDa). All generations were centrifuged once at 1000 × g for 4 min after thorough washing of resin was done in accordance with the manual. Characterization of percent functionalization of the dendrimers with Alexafluor 647 was done by UV-vis using the reported extinction coefficient of 270 000 M^{-1} cm^{-1} at a wavelength of 647 nm.[61] DI water was used as the blank for measurements. A_{647} values of 1.40, 0.928, 0.792, and 0.997 were obtained for G(2), G(3), G(4), and G(6) compounds at 8.61, 4.91, 5.59, and 5.53 µM concentrations, respectively. Concentrations of the dye present in these glycodendrimer solutions were calculated using Beer's law to be 5.19, 3.44, 2.93, and 3.69 µM, respectively. Thus, the ratio of dendrimer: dye was calculated to be 1.7 for G(2), 1.4 for G(3), 1.9 for G(4), and 1.5 for G(6).

Flow cytometry

For flow cytometry, 450 µL of A549 cells (100 000 cells per mL) were seeded in each well of a 24 well plates and incubated for 24 h. Cells were treated with Alexafluor 647 functionalized glycodendrimers and incubated for 2 and 20 h at a final concentration of 0.1 µM and 1.0 µM. Prior to the measurement, cells were washed with PBS and detached using trypsin, transferred to an Eppendorf tube, centrifuged at 140 × g at 4 °C for 4 min, and resuspended in PBS. Fluorescence of the cells was measured in a Attune NxT (Thermo Fisher, Germany), and analysis was done using FlowJo 10.

Confocal microscopy studies of colocalization

For studies of cellular localization using confocal laser scanning microscopy, 270 µL A549 cells (50 000 cells per mL) were seeded in each well of an 8 well ibidi µ-slides in colorless DMEM cell culture medium and cultured overnight with CellLight GFP reagents

targeting lysosomes or early endosomes (CellLight GFP Reagents, BacMam 2.0, Life Technologies GmbH, Darmstadt, Germany). After 22 h, cells were treated with Alexafluor 647 functionalized glycodendrimers and incubated for 2 and 22 h at final concentrations of 0.1 μM and 1.0 μM. Cell nuclei were stained with 1 μg mL^{-1} Hoechst 33342 (Life Technologies GmbH, Darmstadt, Germany). Confocal images were taken with an inverted confocal laser scanning microscope Leica DMI6000CSB SP8 (Leica, Wetzlar, Germany) with a 63×/1.4 HC PL APO CS2 oil immersion objective using the manufacture given LASX software. Image processing was done using Fiji[62] using a macro for batch analysis.

Colocalization analysis was performed using ImageJ (NIH) with custom macros. Images were processed using a two-step automated workflow. First, transfection positive cells regarded as regions of interest (ROIs) were identified by applying an intensity threshold (20 arbitrary units) to the vesicular marker channel, followed by mean filtering with a radius of 25 pixels and a second threshold (25 arbitrary units) to define vesicular structures. ROIs larger than 4000 pixels were selected and extracted from both channels. Subsequently, colocalization analysis was performed using the Colocalization Threshold plugin, implementing the thresholded Manders' coefficient[63] to quantify the fraction of glycodendrimer signal (red channel) colocalizing with vesicular markers (green channel). Analysis was performed on individual frames, and results were concatenated for batch processing.

Apoptosis, viability, and toxicity triplex assay

Cells were added to wells of a 96 well plate so each well contained 9000 cells. The plate was placed in a humidified incubator at 37 °C, 5% CO$_2$ and >80% humidity to allow cells to adhere overnight. The next day, test compounds or controls were added for a final volume of 100 μL per well. A viability control was provided by 0.1% SDS, a cytotoxicity control was provided by ionomycin at a final concentration of 100 μM, and the control for apoptosis was staurosporine at a final concentration of 10 μM. Test compounds were galectin-3 at a final concentration of 6.60 μM, lactose functionalized dendrimers were 220, 140, 60, and 20 μM, for G(2), G(3), G(4), and G(6), respectively. Cells were incubated for 5 h at 37 °C, 5% CO$_2$ and >80% humidity, as per the manufacturer's instructions for the Apotox-Glo Triplex Assay. 20 μL of viability/cytotoxicity reagent containing both GF-AFC Substrate and bis-AAF-R110 were added to each well. The plate was further incubated for 80 min, and fluorescence was measured at 400$_{Ex}$/505$_{Em}$ for viability and 485$_{Ex}$/520$_{Em}$ for cytotoxicity using a Biotek hybrid 1 plate reader. 100 μL of Caspase-Glo 3/7 reagent was added to all wells, and the plate was briefly shaken. Incubation for 30 min was carried out at room temperature protected from light, and luminescence was then measured on the plate reader. A minimum of three replicate experiments were performed.

Acridine orange/ethidium bromide

A549 cells were suspended to 50 000 cells per mL. Cells (15 000 cells per well) were seeded on an 8 well ibidi μ-slide in 300 μL of complete F-12K medium and incubated at 37 °C

and 5% CO$_2$ overnight to adhere. Cells were washed once with 1× PBS and then treated with compounds. All wells had a final volume of 300 μL with equal amounts of 1× PBS, filtered DI water, and complete F-12K medium. Control wells included untreated cells, galectin-3 in 1× PBS (6.6 μM), 0.01% SDS in DI water, and staurosporine (10 μM, stock was dissolved in 50 mM DMSO in DI water). Lactose functionalized G(2), G(3), and G(4) dendrimers were dissolved in complete F-12K medium then added to their respective wells for final concentrations of 220 μM, 140 μM, and 60 μM respectively. G(6) was dissolved in DI water then added to its well for a final concentration of 20 μM. All glycodendrimer wells were treated with a final concentration of 6.6 μM galectin-3. The treated cells were incubated for 5 h at 37 °C and 5% CO$_2$, then stained with 5 μL of acridine orange (AO) and 5 μL ethidium bromide (EB) from their stock solutions made at 100 μg mL^{-1} separately in DI water. Cells were imaged on an inverted confocal laser scanning microscope Leica DMI8 Stellaris (Leica, Bozeman, US) with a 20×/0.75 HC PL APO CS2 dry objective using the manufacturer-provided LASX software. Filters were set for acridine orange (excitation: 488 nm, emission range: 521–542 nm, gain 6.5%) and ethidium bromide (excitation 514 nm, emissions range: 606–650 nm, gain 7.5%).[64] Images were taken immediately, and cells were counted in 10 random images per well. Three biological replicates were obtained for each condition. The same concentrations were repeated using Alexafluor 647 labeled lactose functionalized G(2) and G(6) dendrimers dissolved in DI water (excitation: 650 nm, emission 660–690 nm, gain 2.5%).[64,65]

Phase angle light scattering/dynamic light scattering

Hydrodynamic radii (R_h), zeta potentials, electrophoretic mobility, and conductivity were measured on a Wyatt Möbius DLS instrument. Prior to experimentation, dendrimer solutions were produced and filtered through 0.02 μm filters (Whatman Anotop 25). Zeta potentials, electrophoretic mobility, and conductivity were determined by PALS (phase analysis light scattering) at 10 μM in Millipore water in a 45 μL Dip Cell. Hydrodynamic radii were determined in PBS. DLS source attenuation was allowed for the first scan of a given sample, then auto-attenuation was turned off. Trials interrupted by attenuation were discarded. Reported data, based on measurement in at minimum triplicate, was determined using a regularization fit for an inclusive range of the autocorrelation function.

Statistical analysis

Statistical analysis was performed using the ordinary one way Anova in GraphPad Prism, version 10.2.3. *P = 0.0299, **P < 0.01, ***P = 0.0004 (Fig. 9A), ****P < 0.0001, ns = not significant. Data in graphs are shown as mean with SD.

Results

Toxicity studies using lactose functionalized dendrimers

The toxicity of the four lactose functionalized glycodendrimers shown in Fig. 1 (Table 1) was measured using a fluorescence

viability dye. Three cell lines were investigated: A549 human lung carcinoma cells, DU-145 human prostate carcinoma, and HT-1080 human fibrosarcoma cells. These cell lines were selected for their robustness and endogenous expression of galectin-3 in order from greatest to least: DU-145, A549, then HT-1080. Each cell line was incubated in high concentrations of each generation of lactose functionalized dendrimers (G(2): 390 μM, G(3): 190 μM, G(4): 90 μM or G(6): 35 μM) and Celltox™ dye that fluoresces in the presence of DNA. Fluorescence was recorded at 2 and 24 h. The results were averaged from six replicates of each experiment. The concentration of lactose functionalized dendrimers in the assay was more than double that used in our previously reported assays used for studying cellular aggregation.[56,66] These concentrations of glycodendrimers were selected so that the concentration of lactose was equivalent in each assay, even when the different generation of dendrimer was used with different numbers of lactosides per framework. As shown in Fig. 2, significant dendrimer toxicity was not observed in any of the cell lines tested.

Other researchers have reported cytotoxicity in human epithelial colorectal adenocarcinoma cells at all concentrations studied for G(3) and G(4) cationic or unfunctionalized dendrimers.[67] These researchers also reported a significant decrease in cytotoxicity when the surface of the dendrimers was functionalized with lauroyl or PEG chains and hypothesized that the observed decrease in toxicity was due to the reduced level of positive charge on the surface of the lauroyl and PEG

functionalized dendrimers relative to the unfunctionalized dendrimers with amino termini.[67] As shown in Table 1, the electrophoretic mobilities and zeta potentials for our lactose functionalized glycodendrimers are negligible, but the electrophoretic mobility and the zeta potential for the unfunctionalized G(6)-PAMAM are high. Thus, we conclude that the lactosides effectively shield any remaining cationic ammonium ions.[68]

Toxicity on A549 cells was further assessed using a viability and a toxicity test with the four generations of lactose functionalized glycodendrimers (G(2), G(3), G(4), and G(6)). A viability test was used in which a substrate is only able to enter viable cells; once the substrate is intercellular, proteases are able to cleave and activate a fluorescent tag. Thus, the fluorescence emission is proportional to the number of living cells in the sample. A toxicity test was also performed in which the substrate is only able to be cleaved and activated by proteases released from a dead cell. Ionomycin was used as the toxic control in the toxicity test, and SDS was used as the control for non-viable cells in the viability test. Again, lactose functionalized dendrimers did not have a significantly deleterious impact on cellular viability or toxicity compared to the viable cell controls (Fig. 3).

The viability and toxicity tests were also conducted with exogenously added galectin-3 to assess whether the interaction between the glycodendrimers and galectin-3 impacts cellular viability. Results of the live cell fluorescence assay indicate a
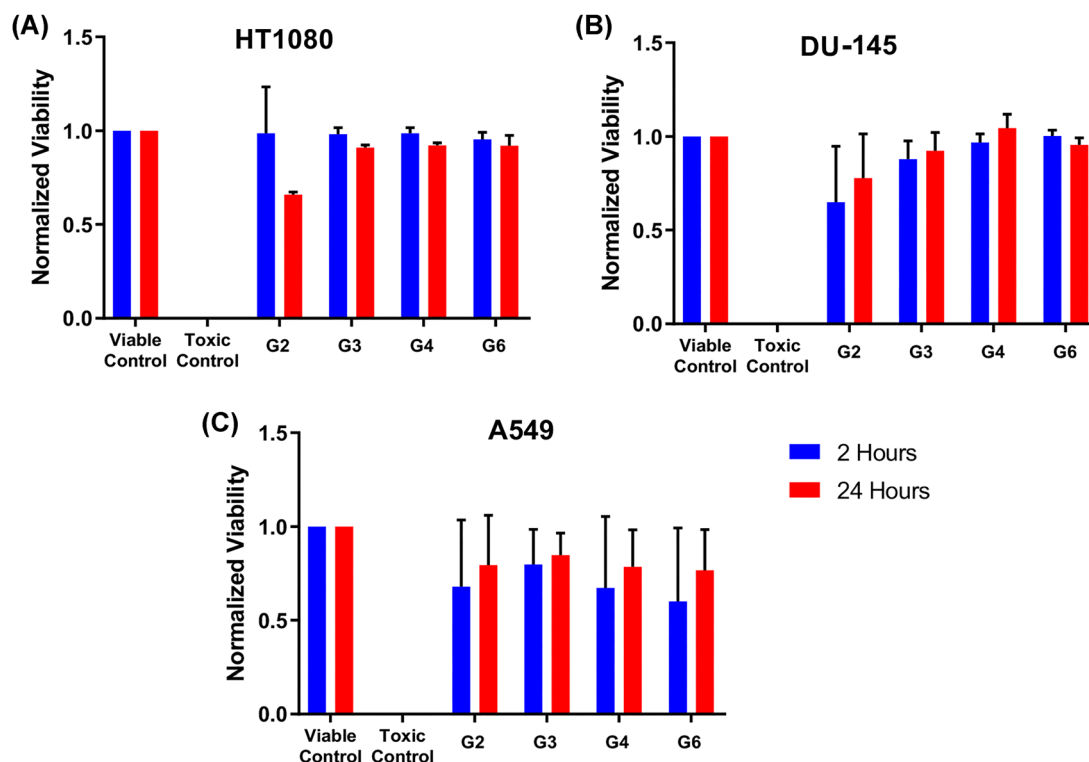

Fig. 2 Toxicity assay using (A) HT1080, (B) DU-145, and (C) A549 cells. Toxicity was compared to untreated cells ("viable control") and cells with lysis buffer added ("toxic control"). Blue bars are measured after 2 h, and red bars are measurements after 24 h of incubation. Error bars demonstrate the standard deviation of 6 replicates.
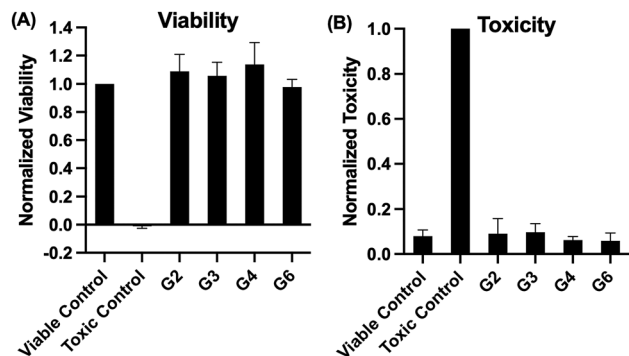
Fig. 3 (A) Viability and (B) toxicity of A549 cells after 5-hour incubation with PBS ("viable control"), lactose functionalized dendrimers (G(2), G(3), G(4), G(6)), or control compounds (A: 0.1% SDS and B: 100 μM ionomycin). Error bars represent standard deviation from a minimum of four replicates.
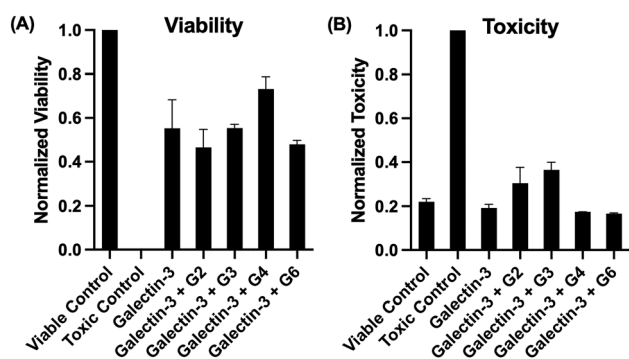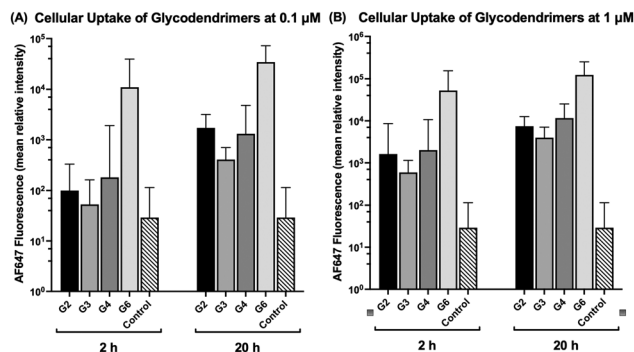

Fig. 5 Cellular uptake of lactose functionalized PAMAM dendrimers by A549 cells is dependent on concentration, exposure time, and dendrimer generation. Uptake of dendrimers at 0.1 μM (A) and 1 μM (B) after 2 and 20 h. Relative intensity is shown on a log 10 scale.

Fig. 4 (A) Viability and (B) toxicity of A549 cells after incubation for 5 hours with control compounds or galectin-3 (6.6 μM) and glycodendrimers (G(2), G(3), G(4), G(6)). Error bars represent standard deviation from three replicate experiments (two replicates for G(4) and G(6) in B).

small decrease in cellular viability when the cells were incubated with galectin-3 and dendrimers for 5 h (Fig. 4A). The decrease in viability is comparable for galectin-3 and for co-additions of glycodendrimer and galectin-3, indicating that the reduction in cellular viability is caused by galectin-3 rather than glycodendrimer or glycodendrimer/galectin-3 aggregates (Fig. 4A). Minor to no significant toxicity was observed in the dead cell fluorescence assay when cells were incubated with galectin-3 and dendrimers compared to the viable control (Fig. 4B).

Cellular uptake of lactose functionalized dendrimers

As noted above, lactose functionalized dendrimers do not exhibit toxic effects in the three cancer cell lines that were tested. In addition to toxicity, the cellular localization of the dendrimers needed to be determined to rationalize their potential effects and interactions with the cells. This is especially important because galectin-3 has both intracellular and extracellular roles in cancer progression.[69,70] Multivalent binding partners for galectin-3 are envisioned to be useful for studies of both extracellular and intracellular functions of the protein, but if cellular uptake of the glycodendrimers is not observed, then modifications will need to be made for studies involving

glycodendrimers and intracellular galectin-3.[71] Nanoparticle surface chemistry and size are known to have a dramatic impact on cellular uptake mechanism and efficiency. Polyethylenimine (PEI) polymers and PAMAM dendrimers feature primary amine endgroups and have been demonstrated to mediate efficient transfection of cells in vivo.[72,73]

Qualitative and quantitative observations of the cellular uptake of the lactose functionalized dendrimers into A549 cells were monitored by laser scanning confocal microscopy and flow cytometry using Alexafluor 647-labeled glycodendrimers. Quantitative studies using flow cytometry show that all generations of glycodendrimers are taken up by the cancer cells (Fig. 5 and Fig. S1–S9 in the ESI†). Lactose functionalized G(2), G(3), and G(4) have similar amounts of uptake, and lactose functionalized G(6) has the most facile uptake. At 1 μM, and at 20 h for both 0.1 μM and 1 μM additions, all generations show significant uptake.

The micrographs shown in Fig. 6 and 7 are color-coded such that the glycodendrimers are magenta, key features of the A549 cell (early endosome (EE) in Fig. 6 or lysosome (Lyso) in Fig. 7) are yellow, colocalization of the two signals is white, and the nuclei are cyan. By labelling early endosomes via GFP transfection, regions of colocalization with the glycodendrimer fluorescence signal were used in an effort to corroborate uptake via endocytosis. Within 2 h of incubation, G(6) can be seen to accumulate around the perimeters of the cells. No significant overlay with the early endosomes is observable. Interestingly, after entering the cell, all generations of glycodendrimers are seen to surround the nucleus after 22 h. The largest glycodendrimer, G(6), had more fluorescence in the micrographs than the other three generations, which is consistent with the results from flow cytometry. The lower generations, while all taken up by the cell, all have very similar micrographs. Additional images including closeups of transfected cells are available as Fig. S10–S42 in the ESI.†

A quantitative comparison of the thresholded Manders' colocalization coefficient 2 (tM2)[63] measuring the fraction of early endosomes that colocalize with the glycodendrimers is shown in Fig. 6I and J. tM2 supports the qualitative observations
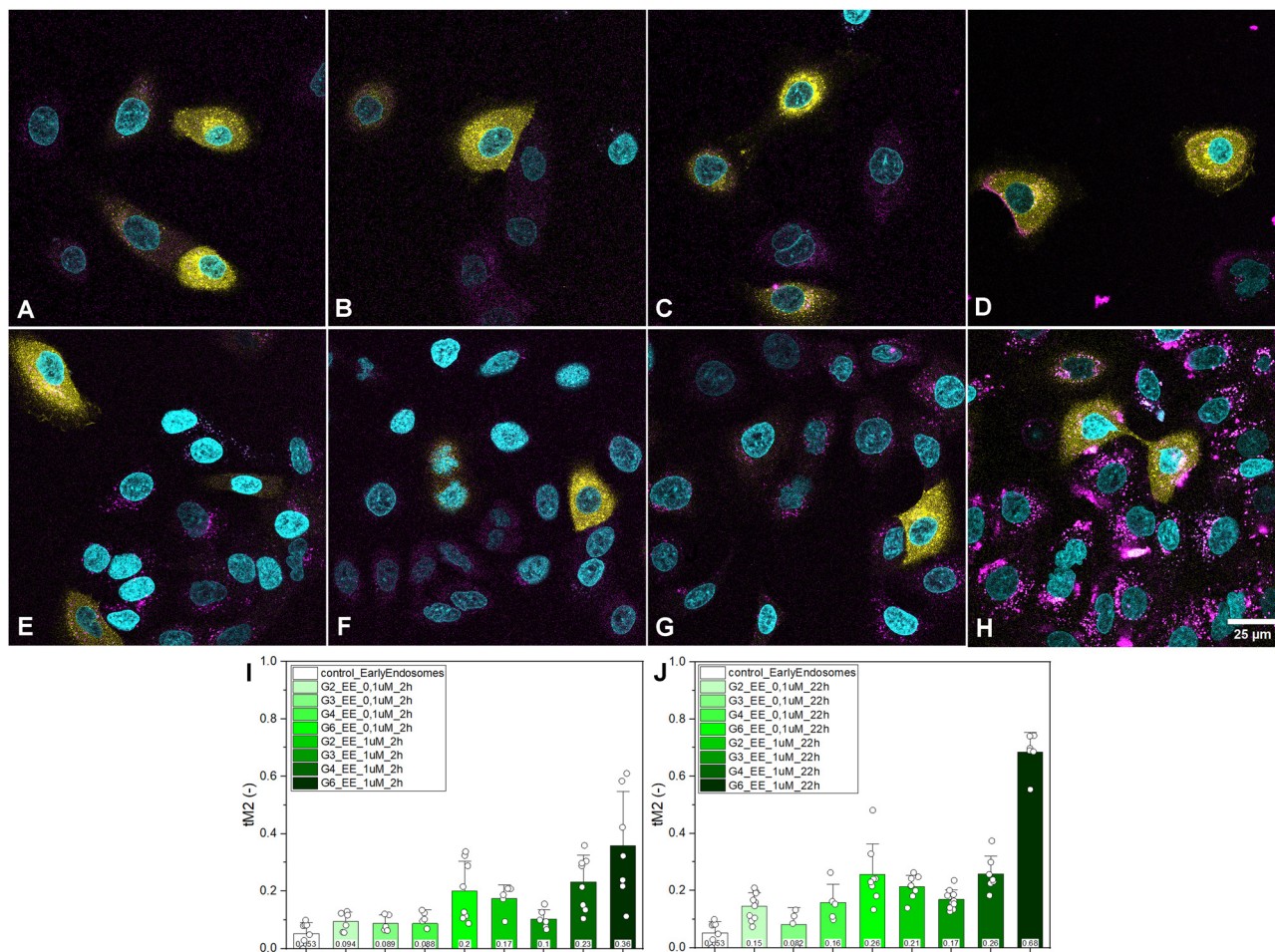
Fig. 6 Confocal laser scanning microscopy Z-stack images of glycodendrimers (0.1 μM) internalized by A549 cells at 2 h (A)–(D) and 22 h (E)–(H). The early endosome (EE) is yellow, Alexafluor 647-labeleddendrimers are magenta, nuclei are cyan. 2 h: (A) G(2), (B) G(3), (C) G(4), and (D) G(6). 22 h: (E) G(2), (F) G(3), (G) G(4), and (H) G(6). Scale bar is 25 μm. Quantitative comparison of the thresholded Manders' colocalization coefficient tM2 for the fraction of EE that colocalizes with the polymer at (I) 2 h and (J) 22 h. The bar charts indicate the mean and standard deviation. The mean value is represented at the bottom of each bar.

described above; G(6) has a much larger tM2 value at 22 h with the early endosome than any other sample. All other glycodendrimers at both 2 h and 22 h have low tM2 values.

Labelling lysosomes *via* GFP transfection was done to try to garner information on the final resting place of the glycodendrimers (Fig. 7). At 2 h, only slight overlap between the lysosome and the glycodendrimers is observed (Fig. 7A–D). At 22 h, lactose functionalized glycodendrimers do appear to have some colocalization with the lysosomes (Fig. 7E–H).

A quantitative comparison of the tM2 values was also calculated for the glycodendrimers and the lysosome. As shown in Fig. 7I and J, the tM2 values are always low at 2 h. tM2 is only greater than 0.5 at 22 h for G(6) at both low and high concentration and for G(4) at the higher concentration. In Fig. 8, the qualitative comparison of the colocalization of red (glycodendrimer) with green (early endosome or lysosome) for the samples with the highest tM2 values also indicates that the most significant colocalization occurs for lactose-functionalized G(6) dendrimer with lysosome at 22 h. Overall, the low amount of colocalization suggests that the glycodendrimers

may take a long time to reach the lysosome and may therefore be quite useful for studies of intracellular galectin-mediated pathways.

Apoptosis assays using glycodendrimers

Galectin-3 is widely believed to play a role in protecting cancer cells from intrinsic apoptosis.[47–49,51] Knowing that our lactose-functionalized glycodendrimers are cell penetrating and non-toxic, we hypothesized that these glycodendrimers could restore apoptosis by diverting galectin-3 from its intracellular binding partners. We tested the induction of apoptosis in A549 cells in the presence of lactose functionalized glycodendrimers with and without exogenous galectin-3 to see if we could abrogate the antiapoptotic effect of galectin-3 using lactose functionalized dendrimers. Intrinsic apoptosis was measured using a luminogenic substance that is activated when cleaved by caspases 3 and 7, well-known players in the apoptotic cascade, and staurosporine was used as a positive control. As shown in Fig. 9A, a small but notable increase in apoptosis occurs (relative to untreated cells) when glycodendrimers are
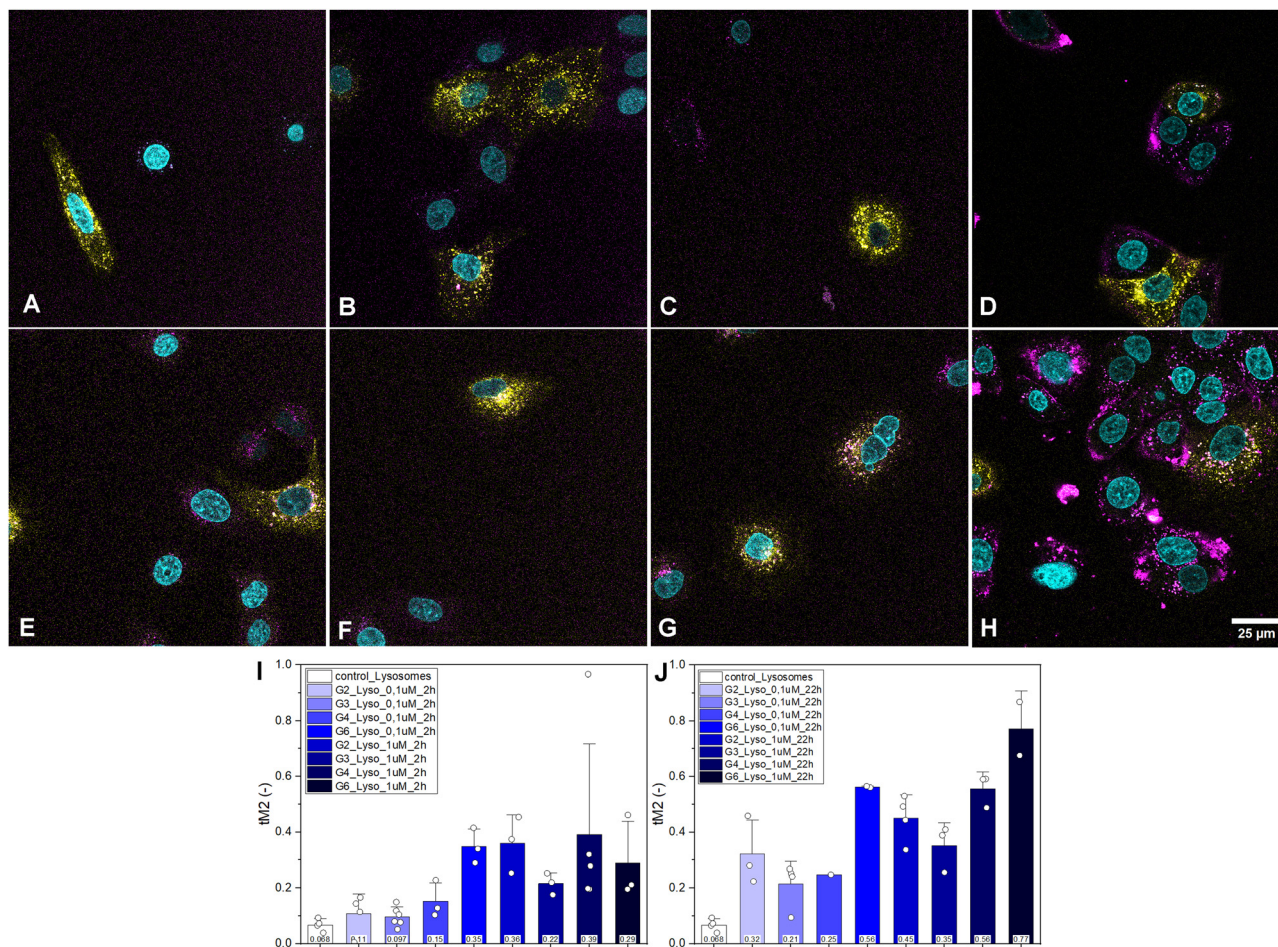
Fig. 7 Confocal laser scanning microscopy Z-stacked images of glycodendrimers (0.1 μM) internalized by A549 cells at 2 h (A)−(D) and 22 h (E)−(H). The lysosome (Lyso) is yellow, Alexafluor 647-labeled dendrimers are magenta, nuclei are cyan, and lysosome/dendrimer overlap is white. 2 h: (A) G(2), (B) G(3), (C) G(4), and (D) G(6). 22 h: (E) G(2), (F) G(3), (G) G(4), and (H) G(6). Scale bar is 25 μm. Quantitative comparison of the thresholded Manders' colocalization coefficient tM2 for the fraction of Lyso that colocalizes with the polymer at (I) 2 h and (J) 22 h. The bar charts indicate the mean and standard deviation. The mean value is represented at the bottom of each bar.

added. One possible straightforward explanation for this is that the glycodendrimers bind endogenous galectin-3 and divert it from its antiapoptotic intracellular processes. Indeed, the glycodendrimers do not have an impact on apoptosis when addition of exogenous galectin-3 is made, suggesting that either the exogenous galectin-3 swamps the system so that galectin-3's role in inhibiting apoptosis is restored, or the exogenous galectin-3 binds the glycodendrimers and reduces their uptake. The former is more likely since uptake of fluorescently labelled glycodendrimers is readily observable in the presence of exogenous galectin-3 (*vide infra*). As shown in Fig. 9B, when exogenous galectin-3 is added with the glycodendrimers, no difference from untreated cells is observed. Significantly less apoptosis occurred than for the staurosporine positive control.

Acridine orange and ethidium bromide cellular investigations by confocal microscopy

Staining with acridine orange and ethidium bromide (AO/EB) was conducted to visually confirm the results of the apoptosis experiment. A549 cells were adhered to glass slides overnight

and were then incubated with control or test compounds for 5 h. The samples were stained with AO/EB and visualized using a confocal microscope. Viable cells displayed green staining throughout the cell, with relatively homogenous fluorescence. Necrotic cells displayed red ethidium bromide staining on their nucleus due to plasma membrane degradation. Apoptotic cells were stained green but with punctate fluorescence in the nucleus due to condensation of DNA and blebbing.

Initially, to validate the procedure and identify phenotypes, viability control experiments using SDS, staurosporine, and exogenous galectin-3 were performed. Untreated cells and cells with only added galectin-3 had a healthy appearance, as shown in Fig. 10A and B, respectively. Cells with SDS and staurosporine appropriately displayed necrosis and apoptosis, as shown in Fig. 10C and D, respectively. These results highlight the main staining and morphological differences used to characterize the cells in this experiment.

Cells in the presence of exogenous galectin-3 and each lactose functionalized dendrimer (G(3), G(4), or G(6)) all appeared to have similar phenotypic distributions, as shown
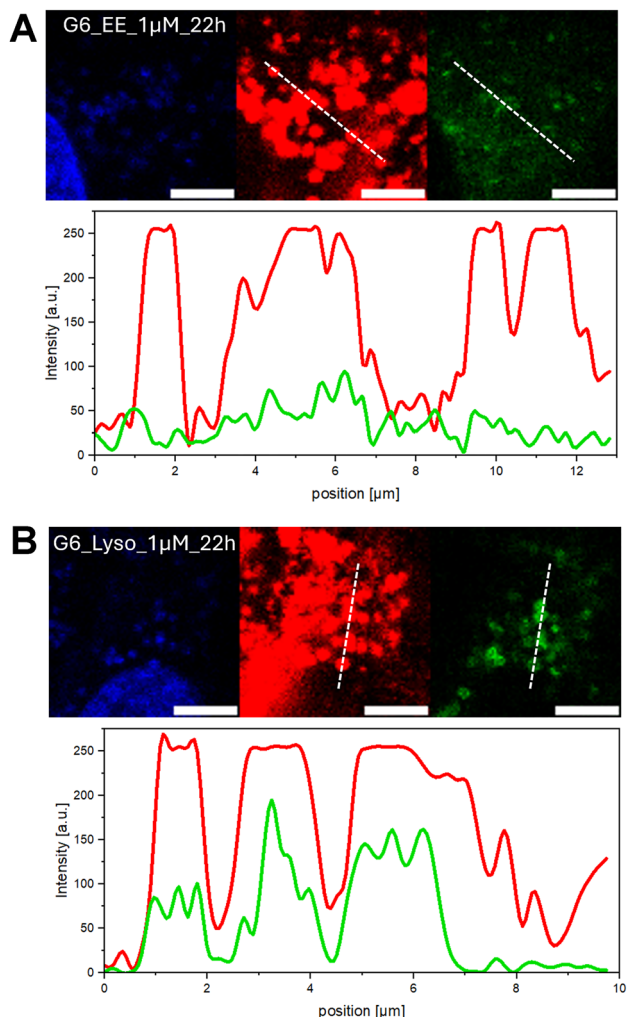
Fig. 8 Qualitative comparison of the colocalization of red (glycodendrimer) and green (early endosome or lysosome) signal based on a line plot and intensity profile for the samples with the highest tM2. G6 1 μM 22 h for early endosome (A) and lysosome (B). Scale bars = 5 μm. The nucleus is blue.

Fig. 9 (A) Apoptosis for A549 cells treated with lactose functionalized dendrimers, staurosporine (positive control), or PBS buffer (viable control) after 5 h incubation; *P = 0.0299, ***P = 0.0004, ****P < 0.0001. (B) Apoptosis for A549 cells treated with lactose functionalized dendrimers and exogenous galectin-3, exogenous galectin-3 alone, staurosporine (positive control), and PBS buffer (viable control) after 5 h incubation. Error bars represent standard deviation from a minimum of three replicates.

added without exogenous galectin-3 (compare Fig. 5, 6, 7 and 11). The sixth generation compounds were taken up significantly better than the second generation compounds when added with galectin-3, just the same as when exogenous galectin-3 was not added. This suggests that glycodendrimer/galectin-3 aggregation at the cell surface does not inhibit cellular uptake of the glycodendrimers. Additional studies aimed at identifying intracellular colocations of glycodendrimers with galectin-3 are ongoing and will be published separately.

Discussion

Functionalized PAMAM dendrimers are attractive substrates for biological applications because of their commercial availability, ease of functionalization, and modularity in terms of size and ligand density.[26,74–76] Multiple amino endgroups are available on the PAMAMs for functionalization, which facilitates the display of multiple ligands on each dendrimer. Dendrimers functionalized with the appropriate ligands can thus utilize the ligands to access multivalent pathways for targeting and release strategies, for solubilization and bioavailability, and for imaging.[68,77] Here, lactose functionalized PAMAM dendrimers are used as a multivalent probe to intercede in galectin-3 mediated anti-apoptotic mechanisms. The utility of all synthetic multivalent systems including glycodendrimers in assays to discern and mediate cellular processes depends on understanding the uptake and toxicity of these compounds.

in Fig. 10F–H. All stages of cell health were observed regardless of dendrimer generation. This agrees with the above results of toxicity and apoptosis, where there was no significant change in toxicity or apoptosis when exogenous galectin-3 was added with the lactose functionalized PAMAM dendrimers, as compared to when galectin-3 was added without glycodendrimers. Only G(2) caused increased toxicity when added with galectin-3, most likely because the cells do not attach to the slide, or to each other, as well in the presence of the G(2)/galectin-3 mixture.[56]

To visualize glycodendrimers, lactose functionalized G(2) and G(6) dendrimers labelled with Alexafluor 647 were used during imaging studies with AO/EB and added galectin-3 (Fig. 11 and Fig. S43 in the ESI†). Fluorescence signals from the glycodendrimers were found both closely around and within the cells for both G(2) (Fig. 11A) and G(6) (Fig. 11B). Thus, uptake of the dendrimers appears to occur both when galectin-3 is exogenously added and when dendrimers are
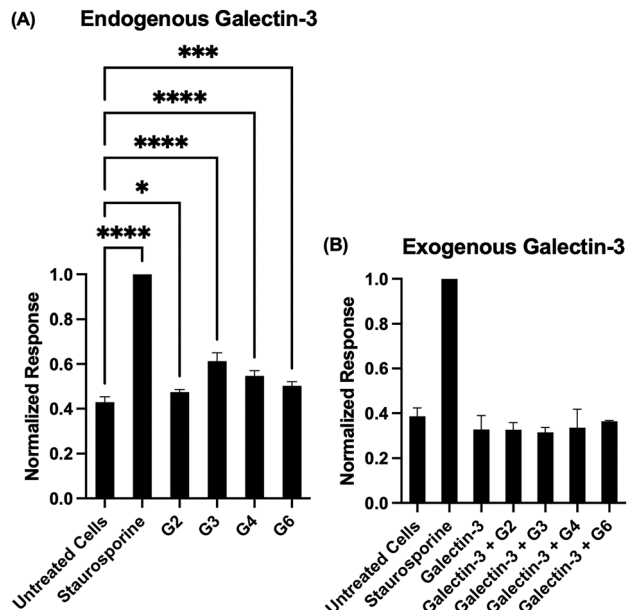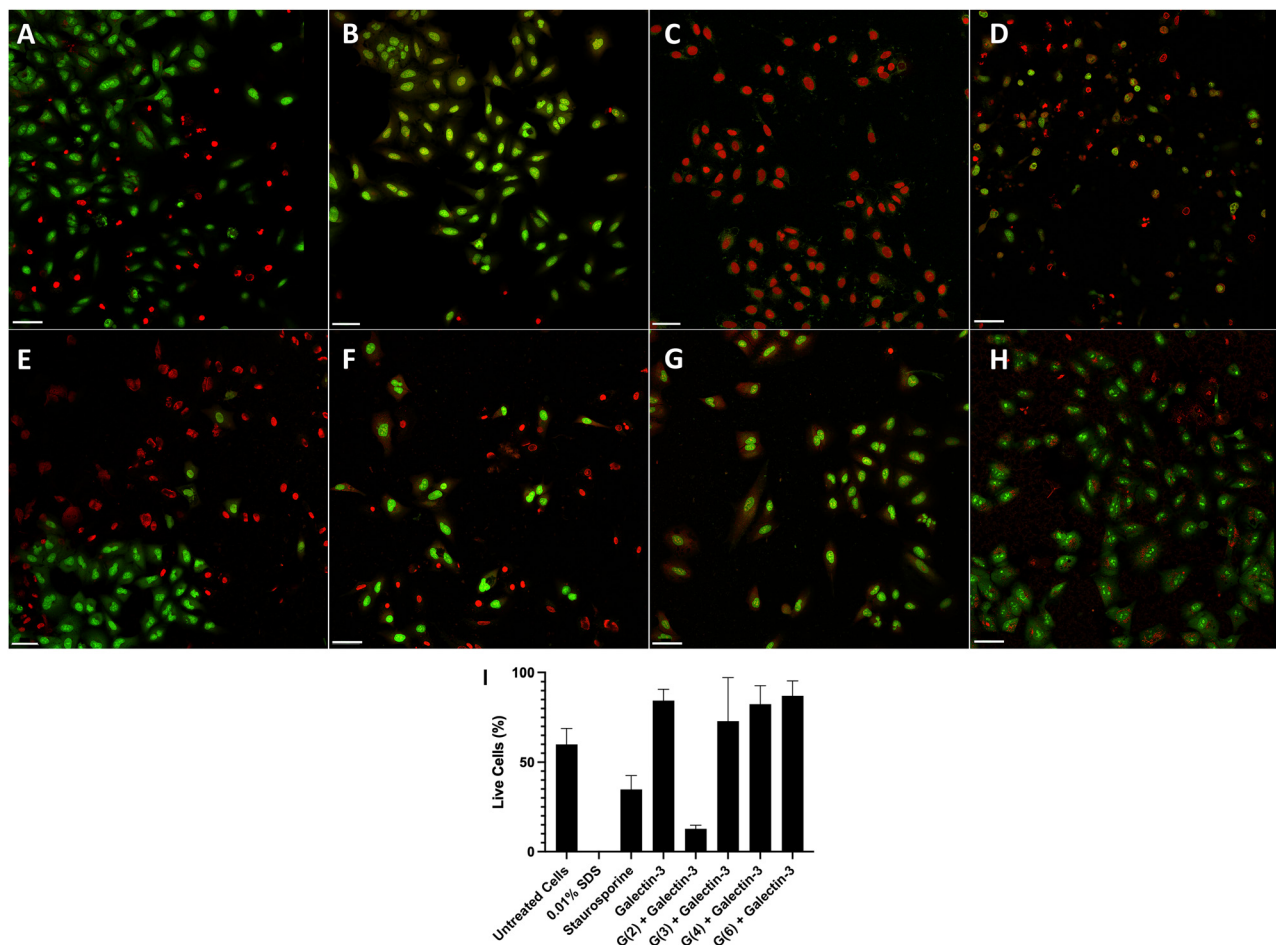
Fig. 10 Confocal microscopy images of A549 after 5 h of incubation with (A) untreated cells, (B) exogenous galectin-3 control conditions, (C) necrosis control (SDS 0.01%), (D) apoptosis control (10 μM staurosporine). For (E)–(H), galectin-3 and lactose functionalized dendrimers were added. (E) G(2), (F) G(3), (G) G(4), and (H) G(6). All samples were stained with acridine orange (green) and ethidium bromide (red). Scale bar is 50 μm. (I) Quantitative comparison of the percentage of the cells that are alive under each of the described conditions.

Importantly, no toxic effects were observed for the lactose functionalized dendrimers in multiple viability and toxicity screens across three cancer cell lines (Fig. 2, 3, 4 and 10). Even after long-term exposure (*i.e.*, incubation for 24 h), significant toxicity was not observed (Fig. 2). Since lactose has been shown to have negligible toxicity,[78] we had hypothesized that lactose functionalized glycodendrimers would be nontoxic.

Although nontoxic, lactose functionalized dendrimers are clearly taken up by cells. Indeed, glycodendrimers functionalized with Alexafluor 647 are taken up efficiently by the cells (Fig. 5). Although Alexafluor labelling of the glycodendrimers could alter their uptake, low fluorescent labelling (less than two Alexafluor 647 moieties per dendrimer) was used to make this unlikely. For example, with an Alexafluor-functionalized virus, no significant difference in the infectivity or replication rate between the labelled and the nonlabelled virus was detected, indicating that uptake was not significantly impacted by Alexafluor labeling.[79]

Although all generations of dendrimers are taken up by the cells, a size dependency was observed, with the largest

dendrimers (G(6)) revealing more fluorescence within the cells than the lower generation dendrimers (G(2), G(3), and G(4)). Extended incubation periods revealed higher fluorescent accumulation in the cell, indicating that more glycodendrimers were present in the cells after 22 h than after 2 h (Fig. 5). Since galectin-3 has long been implicated in prolonged interactions at the cell surface, it seems reasonable that glycodendrimer/galectin-3 interactions at the cell surface cause some of the uptake of the glycodendrimers to be slow. However, since glycolipid–lectin, caveolae, clathrin, and lipid-raft mediated pathways facilitate endocytosis of galectins and glycopolymers, it is also quite reasonable that significant uptake of the glycodendrimers after only two hours is also observed.[39,40] Since G(6) is twice as large as the other glycodendrimers, while G(2), G(3), and G(4) all have similar hydrodynamic radii (see the R_h values in Table 1), it is not surprising that the G(6) glycodendrimer shows somewhat different uptake compared to the other three generations.

For all four generations of glycodendrimers, uptake by the early endosome was low, as shown in Fig. 6. In Fig. 7, a small
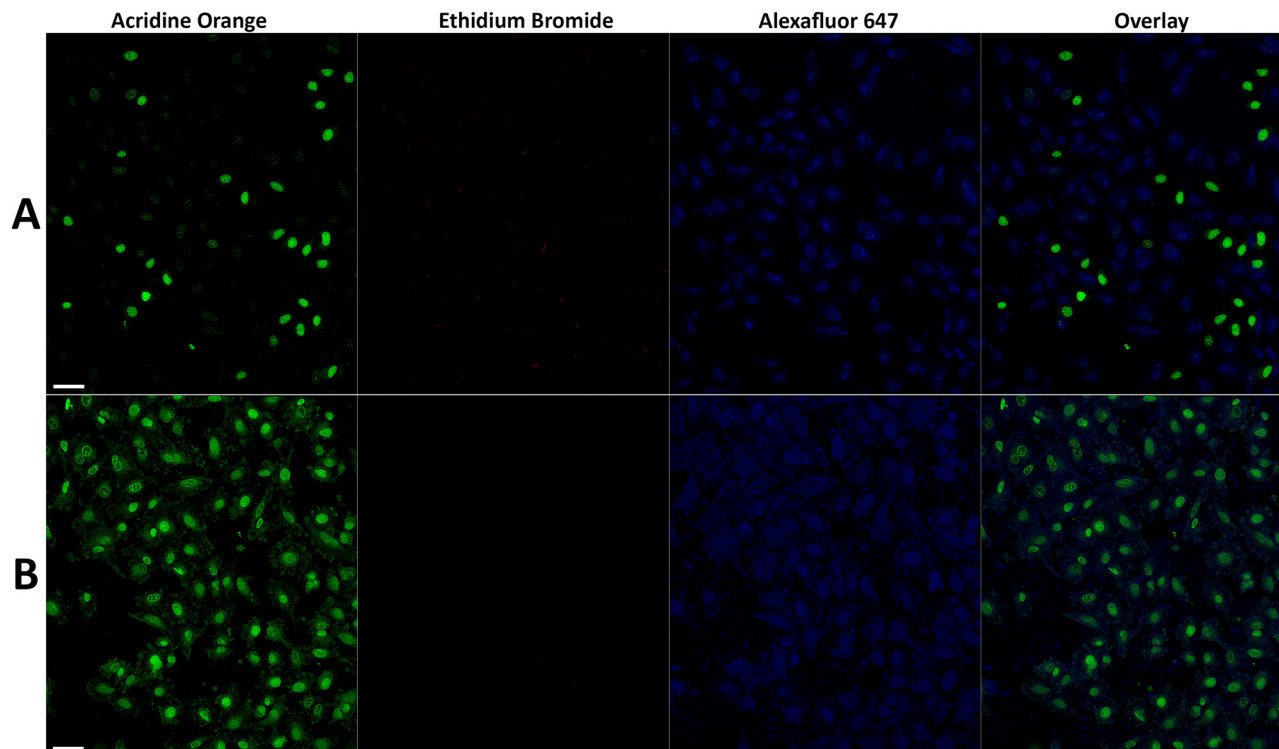
Fig. 11 A549 cells after 5 h incubation with (A) Alexafluor 647-labeled lactose functionalized G(2) glycodendrimers with exogenous galectin-3, and (B) Alexafluor 647-labeled lactose functionalized G(6) glycodendrimers. Cells were stained with AO/EB and visualized by confocal microscopy. A laser intensity of 2.00% was used for imaging G(2) Alexafluor 647, and 0.26% was used for G(6) Alexafluor 647. AO and EB were imaged with the same intensity for both experiments, 1.55% and 2.00%, respectively. Scale bar is 50 μm.

deposition into the lysosome was observable. These studies indicate that the glycodendrimers are not immediately cleared to the lysosome but rather could be available intracellularly for long enough to serve as effective tools for studies of intracellular processes.

The intracellular process that we chose to probe using the glycodendrimers is apoptosis. Galectin-3 has long been proposed to play a key role in protecting cancer cells from chemotherapy-induced apoptosis,[46–49] but the mechanism by which this occurs is not well understood. As shown in Fig. 9A, addition of glycodendrimers to A549 cancer cells causes a small but significant increase in apoptosis for G(3), G(4), and G(6) lactose functionalized dendrimers. No difference between untreated cells and cells treated with G(2) glycodendrimers was observed, perhaps because G(2), by nature of having the lowest number of lactoside endgroups, can bind less galectin-3 per glycodendrimer than the other glycodendrimers. Compared to the amount of apoptosis observed for cells treated with staurosporine, the positive apoptosis control, the dendrimers have only a small effect. It has been reported that exposure of staurosporine to human foreskin fibroblasts leads to cathepsin D accumulation in the cytosol due to staurosporine-induced lysosomal membrane permeabilization in which the contents of the lysosome, including proteases and hydrolases such as cathepsins, are leaked into the cytosol.[80] This brings about the release of cytochrome *c* from the mitochondria, activating caspases and further perpetuating the apoptotic cascade.[81] In our assay, galectin-3 was observed to increase the effectiveness of staurosporine as an inducer of apoptosis (Fig. S44 in the ESI†).

This suggests that perhaps the mechanisms by which staurosporine and galectin-3 activate apoptosis are not the same. The fact that addition of exogenous galectin-3 in the assay eliminates the glycodendrimer-induced increase in apoptosis (Fig. 9B) suggests that glycodendrimers can suppress the anti-apoptotic mechanisms of action of endogenous galectin-3. Previously, we have shown that glycodendrimer/galectin-3 aggregates are readily formed and can alter extracellular processes such as cellular aggregation;[14,56,66] exogenous galectin-3 could also change the localization of both glycodendrimers and galectin-3 if galectin-3/glycodendrimer aggregates are taken up by cells differently than glycodendrimers in the absence of exogenous galectin-3. Addition of exogenous galectin-3 to the system could reduce the uptake of glycodendrimers, making them unavailable intracellularly for interaction with internal endogenous galectin-3. However, this was not observed in the studies described herein.

More studies of the protective role of galectin-3 in the intrinsic apoptosis pathway are needed, and the results presented herein suggest that our compounds are effective materials with which to perform such studies.

Conclusions

The results provided here indicate that lactose functionalized PAMAM dendrimers are nontoxic tools that are useful for the

study of both extra and intracellular galectin-3 mediated processes. These lactose functionalized dendrimers do not exhibit deleterious effects during viability and toxicity assays, and they are taken up well by cancer cells. The glycodendrimers do effect a small increase in cancer cellular apoptosis, and control experiments suggest that the glycodendrimers cause this effect by binding endogenous galectin-3. Since galectins are increasingly emerging as important targets for cancer chemotherapy but their mechanisms of action are not well understood, the need for well-characterized glycodendrimer tools that can be used to study galectin-mediated pathways is significant. Indeed, there are a myriad of biological multivalent interactions, especially in diseases, and glycodendrimers are emerging as important systems to probe and discern these biological interactions.

Author contributions

Conceptualization, M. S. F., M. R. F., S. P. B., K. A., R. H. and M. J. C.; data curation, M. S. F., M. R. F., S. P. B. and M. J. C.; methodology, M. S. F., M. R. F., S. P. B., Y. K., K. A. and M. J. C.; formal analysis, M. S. F., M. R. F., S. P. B., K. A., E. Q., Y. K. and M. J. C.; investigation, M. S. F., M. R. F., S. P. B., K. A., E. Q., R. S. T., W. H. T. and M. J. C.; resources, R. H. and M. J. C.; writing – original draft preparation, M. S. F., M. R. F., S. P. B., K. A. and M. J. C.; writing – review and editing, M. S. F., M. R. F., S. P. B., Y. K., R. H., K. A. and M. J. C.; supervision, K. A., R. H. and M. J. C.; project administration, M. J. C.; funding acquisition, M. J. C.

Data availability

Data supporting this article have been included as part of the ESI.† Any additional data will be made available upon reasonable request.

Conflicts of interest

There are no conflicts to declare.

Acknowledgements

References

1 P. C. Nowell, *Cancer Res.*, 1960, **20**, 462–466.
2 N. Sharon and H. Lis, *Glycobiology*, 2004, **14**, 53R–62R.
3 C. Boscher, J. W. Dennis and I. R. Nabi, *Curr. Opin. Cell Biol.*, 2011, **23**, 383–392.
4 S. Bektas and E. Kaptan, *Life Sci.*, 2024, **346**, 122643.
5 M. F. Troncoso, M. T. Elola, A. G. Blidner, L. Sarrias, M. V. Espelt and G. A. Rabinovich, *J. Biol. Chem.*, 2023, 105400.
6 A. Varki, *Nature*, 2007, **446**, 1023–1029.
7 B. E. Collins and J. C. Paulson, *Curr. Opin. Chem. Biol.*, 2004, **8**, 617–625.
8 M. Mammen, S. K. Choi and G. M. Whitesides, *Angew. Chem., Int. Ed.*, 1998, **37**, 2755–2794.
9 L. L. Kiessling, J. E. Gestwicki and L. E. Strong, *Angew. Chem., Int. Ed.*, 2006, **45**, 2348–2368.
10 M. J. Cloninger, B. Bilgicer, L. Li, S. L. Mangold, S. T. Phillips and M. L. Wolfenden, *Multivalency in Supramolecular Chemistry: From Molecules to Nanomaterials*, John Wiley & Sons Ltd, Chichester, UK, 2012.
11 M. I. Page and W. P. Jencks, *Proc. Natl. Acad. Sci. U. S. A.*, 1971, **68**, 1678–1683.
12 S. Andre, P. J. Ortega, M. A. Perez, R. Roy and H. J. Gabius, *Glycobiology*, 1999, **9**, 1253–1261.
13 N. Seah, P. V. Santacroce and A. Basu, *Org. Lett.*, 2009, **11**, 559–562.
14 C. K. Goodman, M. L. Wolfenden, P. Nangia-Makker, A. K. Michel, A. Raz and M. J. Cloninger, *Beilstein J. Org. Chem.*, 2014, **10**, 1570–1577.
15 Y. M. Chabre and R. Roy, *Adv. Carbohydr. Chem. Biochem.*, 2010, **63**, 165–393.
16 M. Müllerová, M. Hovorková, T. Závodná, L. Stastná, A. Krupková, V. Hamala, K. Nováková, J. Topinka, P. Bojarová and T. Strasák, *Biomacromolecules*, 2023, **24**, 4705–4717.
17 S. Andre, B. C. Liu, H. J. Gabius and R. Roy, *Org. Biomol. Chem.*, 2003, **1**, 3909–3916.
18 S. Andre, R. J. Pieters, I. Vrasidas, H. Kaltner, L. Kuwabara, F. T. Liu, R. M. J. Liskamp and H. J. Gabius, *ChemBioChem*, 2001, **2**, 822–830.
19 I. Vrasidas, S. Andre, P. Valentini, C. Bock, M. Lensch, H. Kaltner, R. M. J. Liskamp, H. J. Gabius and R. J. Pieters, *Org. Biomol. Chem.*, 2003, **1**, 803–810.
20 R. Roy, T. C. Shiao and K. Rittenhouse-Olson, *Braz. J. Pharm. Sci.*, 2013, **49**, 2013, DOI: **10.1590/S1984-8250201300070 0008**.
21 L. Abbassi, Y. Chabre, N. Kottari, A. Arnold, S. André, J. Josserand, H. Gabius and R. Roy, *Polym. Chem.*, 2015, **6**, 7666–7683.
22 M. Gorzkiewicz, K. Sztandera, I. Jatczak-Pawlik, R. Zinke, D. Appelhans, B. Klajnert-Maculewicz and L. Pulaski, *Biomacromolecules*, 2018, **19**, 1562–1572.

23 D. A. Tomalia, H. Baker, J. Dewald, M. Hall, G. Kallow, S. Martin, J. Roeck, J. Ryder and P. Smith, *Polym. J.*, 1985, **17**, 117–132.

24 D. A. Tomalia and H. D. Durst, *Genealogically Directed Synthesis: Starburst/Cascade Dendrimers and Hyperbranched Structures*, Springer-Verlag, Berlin, 1993.

25 G. R. Newkome, C. N. Moorefield and F. Vögtle, *Dendrimers and Dendrons: Concepts, Syntheses, Applications*, Wiley-VCH, Weinheim, 2001.

26 M. J. Cloninger, *Curr. Opin. Chem. Biol.*, 2002, **6**, 742–748.

27 M. Reynolds and S. Perez, *C. R. Chim*, 2011, **14**, 74–95.

28 L. L. Kiessling and R. A. Splain, *Ann. Rev. Biochem.*, 2010, **79**, 619–653.

29 A. P. Dias, S. d S. Santos, J. V. da Silva, R. Parise-Filho, E. I. Ferreira, O. El Seoud and J. Giarolla, *Int. J. Pharm.*, 2020, **573**, 118814, DOI: 10.1016/j.ijpharm.2019.118814.

30 M. Martínez-Bailén, J. Rojo and J. Ramos-Soriano, *Chem. Soc. Rev.*, 2023, **52**, 536–572.

31 W. B. Turnbull and J. F. Stoddart, *J. Biotechnol.*, 2002, **90**, 231–255.

32 A. Bernardi, J. Jiménez-Barbero, A. Casnati, C. De Castro, T. Darbre, F. Fieschi, J. Finne, H. Funken, K.-E. Jaeger, M. Lahmann, T. Lindhorst, M. Marradi, P. Messner, A. Molinaro, P. Murphy, C. Nativi, S. Oscarson, S. Penadés, F. Peri, R. J. Pieters, O. Renaudet, J.-L. Reymond, B. Richichi, J. Rojo, F. Sansone, C. Schaffer, W. B. Turnbull, T. Velasco-Torrijos, S. Vidal, S. Vincent, T. Wennekes, H. Zuilhof and A. Imberty, *Chem. Soc. Rev.*, 2013, **42**, 4709–4727.

33 T. Lindhorst, *Host Guest Chem.*, 2002, **218**, 201–235.

34 K. V. Marino, A. J. Cagnoni, D. O. Croci and G. A. Rabinovich, *Nat. Rev. Drug Discovery*, 2023, **22**, 295–316.

35 P. Navarro, N. Martinez-Bosch, A. G. Blidner and G. A. Rabinovich, *Clin. Cancer Res.*, 2020, **26**, 6086–6101.

36 C. M. Arthur, M. D. Baruffi, R. D. Cummings and S. R. Stowell, in *Galectins: Methods and Protocols*, ed. S. R. Stowell and R. D. Cummings, 2015, vol. 1207, pp. 1–35.

37 G. G. Caballero, H. Kaltner, T. J. Kutzner, A. K. Ludwig, J. C. Manning, S. Schmidt, F. Sinowatz and H. J. Gabius, *Histol. Histopathol.*, 2020, **35**, 509–539.

38 R. Nehme and Y. St-Pierre, *Front. Immunol.*, 2023, **14**, DOI: 10.3389/fimmu.2023.1269391.

39 L. Johannes, M. Shafaq-Zadah, E. Dransart, C. Wunder and H. Leffler, *Cold Spring Harbor Perspect. Biol.*, 2024, **16**, a041398.

40 L. C. Nelemans and L. Gurevich, *Materials*, 2020, **13**, 366.

41 M. Vlachova, V. N. Tran, J. Cerveny, F. Dolnicek, L. Petraskova, H. Pelantova, O. Kundrat, J. Cvacka, Z. Bosakova, V. Kren, P. Lhotak, J. Viktorova and P. Bojarova, *Chem. Commun.*, 2023, **59**, 10404–10407.

42 D. Vrbata, M. Filipova, M. R. Tavares, J. Cerveny, M. Vlachova, M. Sirova, H. Pelantova, L. Petraskova, L. Bumba, R. Konefal, T. Etrych, V. Kren, P. Chytil and P. Bojarova, *J. Med. Chem.*, 2022, **65**, 3866–3878.

43 R. Yokoyama, T. Taharabaru, T. Nishida, Y. Ohno, Y. Maeda, M. Sato, K. Ishikura, K. Yanagihara, H. Takagi, T. Nakamura, S. Ito, S. Ohtsuki, H. Arima, R. Onodera, T. Higashi and K. Motoyama, *J. Controlled Release*, 2020, **328**, 722–735.

44 P. Sun, Y. He, M. Lin, Y. Zhao, Y. Ding, G. Chen and M. Jiang, *ACS Macro Lett.*, 2014, **3**, 96–101.

45 Y. Hayashi, Y. Mori, S. Yamashita, K. Motoyama, T. Higashi, H. Jono, Y. Ando and H. Arima, *Mol. Pharmaceutics*, 2012, **9**, 1645–1653.

46 S. Sciacchitano, L. Lavra, A. Morgante, A. Ulivieri, F. Magi, G. P. De Francesco, C. Bellotti, L. B. Salehi and A. Ricci, *Int. J. Mol. Sci.*, 2018, **19**, 379.

47 K. Seyrek, M. Richter and I. N. Lavrik, *Cell Death Differ.*, 2019, **26**, 981–993.

48 Y. Harazono, K. Nakajima and A. Raz, *Cancer Metastasis Rev.*, 2014, **33**, 285–294.

49 D. Chauhan, G. L. Li, K. Podar, T. Hideshima, P. Neri, D. L. He, N. Mitsiades, P. Richardson, Y. Chang, J. Schindler, B. Carver and K. C. Anderson, *Cancer Res.*, 2005, **65**, 8350–8358.

50 J. Kopitz, S. Vertesy, S. Andre, S. Fiedler, M. Schnoelzer and H.-J. Gabius, *Biochimie*, 2014, **104**, 90–99.

51 A. C. F. Cardoso, L. N. D. Andrade, S. O. Bustos and R. Chammas, *Front. Oncol.*, 2016, **6**, 127.

52 N. Ahmad, H. J. Gabius, S. Andre, H. Kaltner, S. Sabesan, R. Roy, B. C. Liu, F. Macaluso and C. F. Brewer, *J. Biol. Chem.*, 2004, **279**, 10841–10847.

53 N. Ahmad, H. J. Gabius, S. Sabesan, S. Oscarson and C. F. Brewer, *Glycobiology*, 2004, **14**, 817–825.

54 B. N. Stillman, D. K. Hsu, M. Pang, C. F. Brewer, P. Johnson, F. T. Liu and L. G. Baum, *J. Immunol.*, 2006, **176**, 778–789.

55 X. Gao, J. Liu, X. Liu, L. Li and J. Zheng, *Cancer Metastasis Rev.*, 2017, **36**, 367–374.

56 A. K. Michel, P. Nangia-Makker, A. Raz and M. J. Cloninger, *ChemBioChem*, 2014, **15**, 2106–2112.

57 A. I. Markowska, F.-T. Liu and N. Panjwani, *J. Exp. Med.*, 2010, **207**, 1981–1993.

58 P. Nangia-Makker, V. Balan and A. Raz, *Cancer Microenviron.*, 2008, **1**, 43–51.

59 F. T. Liu and G. A. Rabinovich, *Nat. Rev. Cancer*, 2005, **5**, 29–41.

60 M. C. Vladoiu, M. Labrie and Y. St-Pierre, *Int. J. Oncol.*, 2014, **44**, 1001–1014.

61 AAT Bioquest, Quest Database™ Extinction Coefficient [Alexa Fluor 647], (accessed March 8, 2025).

62 J. Schindelin, I. Arganda-Carreras, E. Frise, V. Kaynig, M. Longair, T. Pietzsch, S. Preibisch, C. Rueden, S. Saalfeld, B. Schmid, J.-Y. Tinevez, D. J. White, V. Hartenstein, K. Eliceiri, P. Tomancak and A. Cardona, *Nat. Methods*, 2012, **9**, 676–682.

63 E. Manders, F. Verbeek and J. Aten, *J. Microsc.*, 1993, **169**, 375–382.

64 S. M. Smith, D. Ribble, N. B. Goldstein, D. A. Norris and Y. G. Shellman, *Lab. Methods Cell Biol.: Biochem. Cell Cult.*, 2012, **112**, 361–368.

65 ThermoFisher Scientific, Excitation and Emission Dye Profiles [Alexa Fluor 647] (accessed March 8, 2025).

66 J. H. Ennist, H. R. Termuehlen, S. P. Bernhard, M. S. Fricke and M. J. Cloninger, *Bioconjugate Chem.*, 2018, **29**, 4030–4039.

67 R. Jevprasesphant, J. Penny, R. Jalal, D. Attwood, N. B. McKeown and A. D'Emanuele, *Int. J. Pharm.*, 2003, **252**, 263–266.

68 H. W. VanKoten, W. M. Dlakic, R. Engel and M. J. Cloninger, *Mol. Pharm.*, 2016, **13**, 3827–3834.

69 F. T. Liu, R. J. Patterson and J. L. Wang, *Biochim. Biophys. Acta, Gen. Subj.*, 2002, **1572**, 263–273.

70 A. U. Newlaczyl and L.-G. Yu, *Cancer Lett.*, 2011, **313**, 123–128.

71 E. A. Partridge, C. Le Roy, G. M. Di Guglielmo, J. Pawling, P. Cheung, M. Granovsky, I. R. Nabi, J. L. Wrana and J. W. Dennis, *Science*, 2004, **306**, 120–124.

72 M. Piest and J. F. J. Engbersen, *J. Controlled Release*, 2010, **148**, 83–90.

73 O. Boussif, F. Lezoualch, M. A. Zanta, M. D. Mergny, D. Scherman, B. Demeneix and J. P. Behr, *Proc. Natl. Acad. Sci. U. S. A.*, 1995, **92**, 7297–7301.

74 A. M. Caminade and C. O. Turrin, *J. Mater. Chem. B*, 2014, **2**, 4055–4066.

75 A. P. Sherje, M. Jadhav, B. R. Dravyakar and D. Kadam, *Int. J. Pharm.*, 2018, **548**, 707–720.

76 A. K. Patri and E. Simanek, *Mol. Pharm.*, 2012, **9**, 341.

77 R. E. Wang, F. Costanza, Y. H. Niu, H. F. Wu, Y. G. Hu, W. Hang, Y. Q. Sun and J. F. Cai, *J. Controlled Release*, 2012, **159**, 154–163.

78 P. Baldrick and D. G. Bamford, *Food Chem. Toxicol.*, 1997, **35**, 719–733.

79 S. Zhang, H. Tan, B. Hanson and E. Ooi, *J. Virol. Methods*, 2010, **167**, 172–177.

80 S. Ivanova, U. Repnik, L. Bojic, A. Petelin, V. Turk and B. Turk, *Methods Enzymol.*, 2008, **442**, 183–199.

81 A. C. Johansson, H. Steen, K. Ollinger and K. Roberg, *Cell Death Differ.*, 2003, **10**, 1253–1259.